symmetry

MDPI

Article

Permeability Characteristics and Strength Degradation Mechanisms of Drilling Fluid Invading Bedding-Shale Fluid

Guiquan Wang [1,2], Fenfen Li [1], Yu Suo [1,3,4,5,*], Cuilong Kong [2], Xiaoguang Wang [6] and Lingzhi Zhou [6]

[1] School of Petroleum Engineering, Northeast Petroleum University, Daqing 163318, China; wangguiquan@petrochina.com.cn (G.W.); ff123_2023@163.com (F.L.)
[2] Daqing Oilfield Production Technology Institute, Daqing Oilfield Limited Company, Daqing 163458, China; xj01_kongcl@petrochina.com.cn
[3] Key Laboratory of Continental Shale Hydrocarbon Accumulation and Efficient Development, Northeast Petroleum University, Ministry of Education, Daqing 163318, China
[4] Postdoctoral Resource Center, Daqing Oilfield Limited Company, Daqing 163458, China
[5] Heilongjiang Province Key Laboratory of Oil and Gas Reservoir Fracturing and Evaluation, Daqing 163318, China
[6] Daqing Oilfield Downhole Services Company, Daqing 163458, China; xj_wangxiaog@petrochina.com.cn (X.W.); jx_zhoulz@petrochina.com.cn (L.Z.)
* Correspondence: sycup09@163.com

Abstract

The development of shale bedding and fractures exacerbates the invasion of drilling fluid, leading to significant reservoir damage. This article elucidates the strength degradation behavior of shale with bedding orientations of 0° and 90° under drilling fluid immersion, as determined through triaxial compression experiments. An improved Hooke–Brown anisotropic strength criterion has been established to quantitatively characterize the degradation effects. Additionally, a dynamic mechanism of pore pressure accumulation was simulated. The research findings indicate the following: (1) As the intrusion pressure increases from 6 MPa to 8 MPa, the penetration depth significantly increases. In the horizontal bedding direction (0°), cracks dominate the flow mode, resulting in a sudden drop in strength; (2) An increase in bedding density or opening exacerbates the degree of invasion and strength degradation in the horizontal bedding direction, with a degradation rate exceeding 40%. In contrast, the vertical bedding direction is influenced by permeability anisotropy and crack blockage, leading to limited seepage and minimal degradation. By optimizing the dosage of emulsifiers and other treatment agents through orthogonal experiments, a low-viscosity, high-shear-strength plugging oil-based drilling fluid system was developed, effectively reducing the invasion depth of the drilling fluid by over 30%. The primary innovations of this article include the establishment of a quantitative model for Reynolds number degradation for the first time, which elucidates the mechanism of accelerated crack propagation during turbulent transition (when the Reynolds number exceeds the critical value of 10). Additionally, a novel method for synergistic control between sealing and rheology is introduced, significantly decreasing the degradation rate of horizontal bedding. Furthermore, the development of the Darcy–Forchheimer partitioning algorithm addresses the issue of prediction bias exceeding 15% in high-Reynolds-number regions (Re > 30). The research findings provide a crucial theoretical foundation and data support for the optimized design of drilling fluids.

Keywords: bedding shale; drilling fluid invasion; strength degradation; failure criterion; pore pressure

check for updates

Academic Editor: Vasilis K. Oikonomou

Received: 13 May 2025
Revised: 18 June 2025
Accepted: 19 June 2025
Published: 21 June 2025

Citation: Wang, G.; Li, F.; Suo, Y.; Kong, C.; Wang, X.; Zhou, L. Permeability Characteristics and Strength Degradation Mechanisms of Drilling Fluid Invading Bedding-Shale Fluid. *Symmetry* **2025**, *17*, 981. https://doi.org/10.3390/sym17070981

Copyright: © 2025 by the authors. Licensee MDPI, Basel, Switzerland. This article is an open access article distributed under the terms and conditions of the Creative Commons Attribution (CC BY) license (https://creativecommons.org/licenses/by/4.0/).

1. Introduction

In practical drilling operations, vibrations in the drill string can induce fractures in shale reservoirs, creating pathways for drilling fluid to invade the formation. This invasion allows the drilling fluid to interact with the shale reservoir, thereby altering the mechanical properties of the bedding shale and impacting wellbore stability. When drilling fluid filtrate penetrates the formation along bedding planes or weak surfaces of the shale, the water absorption and swelling capacities of various clay minerals exhibit significant directional variation, demonstrating pronounced anisotropy. Furthermore, the hydration and swelling rates of different clay particles differ, resulting in varying swelling pressure differentials. This imbalance of internal stresses within the formation diminishes the strength of the shale, making it susceptible to wellbore instability along bedding planes and weak surfaces [1].

Extensive rock mechanics experiments and field evaluations have been conducted by both domestic and international researchers. These studies have confirmed the significant impact of bedding planes and weak surfaces on the stability of shale wellbores. Furthermore, the invasion of drilling fluid filtrate into the formation increases pore pressure and reduces rock strength, exacerbating wellbore instability. On one hand, numerous scholars have conducted research on the anisotropic characteristics of shale strength. Zheng et al. [2] evaluate the anisotropic mechanical properties of shale by tri-axial tests and predict shale anisotropic properties by well-logging data interpretation. The shale mechanical properties of different bedding-plane orientations were studied. Lee et al. [3] derived an analytical model for shale-wellbore stability considering strength anisotropy. This method pre-calculates the safety of the wellbore at various positions, enabling the optimization of the drilling trajectory to prevent wellbore collapse. Zhang et al. [4] considered the influence of bedding and anisotropy, establishing an improved wellbore stability evaluation model that accounts for the time-dependent characteristics of rock compressive strength and developed a logging data-based evaluation method. Ahmed et al. [5] analyzed the transmission mechanism of water in shale and established an anisotropic shale-wellbore pressure transfer model based on non-equilibrium thermodynamics. They investigated the effects of formation anisotropy and well inclination on wellbore failure, proposing appropriate drilling fluid densities based on well inclination and azimuth by incorporating strength anisotropy into geomechanical models. Asaka et al. [6] conducted an anisotropic wellbore stability analysis for an offshore gas field. They calculated stress concentrations around circular boreholes in anisotropic shale using the Amadei solution and derived induced pore pressures from Skempton parameters based on anisotropic poroelastic theory. Ma et al. [7] considered the influence of rock anisotropy, derived a stress distribution model for vertical wellbores, and established a fracture pressure calculation method for anisotropic formations, analyzing the effects of bedding orientation, degree of anisotropy, in situ stress, and pore pressure. Li et al. [8] experimentally determined the anisotropic elastic and strength parameters of Longmaxi shale in the deep southern Sichuan Basin. They analyzed bedding orientation using imaging logs and determined the magnitude and orientation of in situ stress through laboratory experiments and logging data, establishing an anisotropic shale-wellbore collapse pressure model and analyzing collapse pressures under various formation conditions. Yan et al. [9] think that the establishment of an appropriate rock physics model has a direct impact on the accurate determination of rock anisotropy parameters and P-S wave velocity. Luo et al. [10] found that the mechanical properties of shale exhibit significant anisotropy and confining pressure effects. The lubricating effect of oil-based drilling fluids on bedding planes enhances anisotropy, leading to shear failure along these planes, with failure modes influenced by bedding orientation.

On the other hand, some scholars have conducted extensive research on the changes in the mechanical properties of shale due to drilling fluid invasion. Zhou et al. [11] determined

the mechanical properties of the shale before and after immersion in drilling fluid. Based on the experimental results, combined with the spring combination model and fault activation theory, a quantitative evaluation of fault activation risk was conducted. Wang et al. [12] used nuclear magnetic resonance (NMR) scanning, while we measured the intrusion depth at layer joints while eliminating the interference from solid particles in the drilling fluid during weighing. Liu et al. [13] conducted mechanical tests on Longmaxi shale before and after immersion in drilling fluid. They discovered that bedding fractures in Longmaxi shale are well-developed, and the effects of drilling fluid immersion significantly impact the mechanical strength of bedding shale, with varying degrees of strength reduction observed in shale samples with different bedding angles. Geng et al. [14] examined the changes in mechanical parameters, such as peak strength, elastic modulus, and Poisson's ratio of shale, under the weakening effects of drilling fluid. Utilizing the strain equivalence principle and Weibull statistical distribution theory, they established a damage constitutive model for rock subjected to the combined effects of drilling fluid immersion and uniaxial loading. Wang et al. [15] investigated evaluation methods for assessing the degree and impact of drilling fluid invasion in ultra-low-permeability sandstone reservoirs. Their approach integrated dynamic analysis, seepage theory, and material balance principles, combining both dynamic and static analyses. Dong et al. [16] developed a thermo–hydro–mechanical coupling model that describes the geophysical field characteristics and wellbore failure. Their research demonstrated that drilling fluid invasion results in stress and strain concentration around the wellbore, which adversely affects wellbore stability. Deng [17] formulated a theoretical model to predict wellbore stress in shale formations, taking into account the combined effects of seepage and hydration. He employed an implicit difference method to solve the model, thereby obtaining variations in wellbore stress under different conditions. Additionally, he established a collapse pressure prediction model for shale wellbores, also considering the combined effects of seepage and hydration. Li et al. [18,19] used the DEA–SBM model and GML index to conduct static and dynamic evaluations of carbon emission efficiency, and the Tobit model was used to analyze the factors affecting this efficiency from both internal and external perspectives. They also determined the depth of drilling fluid invasion into shale under varying confining pressures and displacement times through displacement experiments and nuclear magnetic resonance (NMR) scanning. They established a mathematical relationship between the depth of drilling fluid invasion and factors such as invasion time, invasion pressure differential, confining pressure, bedding angle, and drilling fluid viscosity. This relationship provides a foundation for the subsequent determination of collapse pressure and collapse cycles in bedding shale. Suo et al. [20] examined the invasion patterns of drilling fluid in laminated shale, conducting displacement experiments and NMR scanning to ascertain the depth of drilling fluid invasion into laminated shale at different displacement times. Based on their experimental findings, they developed a new mathematical model for laminated shale that incorporates the effects of drilling fluid invasion. Wang et al. [21] simulated the process of drilling fluid permeating layered shale through fluid invasion experiments, deriving the variation patterns of mechanical parameters in the shale matrix and bedding planes. They analyzed the effects of different types of drilling fluids, formation bedding, well inclination, well azimuth, formation dip angle, and drilling cycle on collapse pressure and collapse area. Ma et al. [22] found that drilling fluid invades the formation along bedding planes during seepage, which reduces the cohesion and internal friction angle of the bedding planes. This alteration makes the wellbore rock more susceptible to sliding along the bedding planes, thereby increasing the risk of wellbore collapse.

While existing studies predominantly investigate either the anisotropic mechanical properties of shale or the isolated effects of drilling fluid invasion on wellbore stability, the

coupled interactions between these factors remain insufficiently explored. In bedding-shale reservoirs, prevalent bedding fractures facilitate drilling fluid invasion, which subsequently degrades the rock's mechanical integrity and precipitates wellbore instability. To address this knowledge gap, this study systematically examines the mechanical responses and failure mechanisms of bedding shale under drilling fluid exposure through uniaxial and triaxial compression tests conducted at varying bedding orientations. The experimental results elucidate the strength degradation mechanisms induced by fluid-shale interactions, providing a theoretical foundation for optimizing drilling fluid systems in bedding-shale formations.

2. Experimental Study on the Compressive Strength of Deep-Bedded Shale Under Drilling Fluid Invasion

2.1. Core Sampling and Experimental Design

To investigate the influence of drilling fluid invasion on the strength characteristics of bedded shale in deep formations, a systematic experimental program was designed to evaluate compressive strength under varying confining pressures and different durations of fluid invasion. The experimental matrix comprises two test series: (1) Compressive strength tests conducted at a confining pressure of 30 MPa with oil-based drilling fluid invasion durations of 0 h, 24 h, 48 h, 72 h, 96 h, and 120 h; (2) Compressive strength assessments at a 72 h invasion duration under three confining pressures (0 MPa, 15 MPa, and 30 MPa).

Due to the development of shale bedding and fractures, the success rate of traditional methods for preparing samples is low. The wire cutting method was employed to prepare standard rock cores measuring 25 mm × 50 mm along the 0° and 90° directions of the shale-bedding plane. Both ends of the sample were cut flat and polished to achieve an aspect ratio of approximately 2. The parallelism of the upper and lower end faces of the sample must be maintained within ±0.03 mm. To ensure the accuracy of the experiment, three samples were prepared for each angle. The core sample is illustrated in Figure 1.

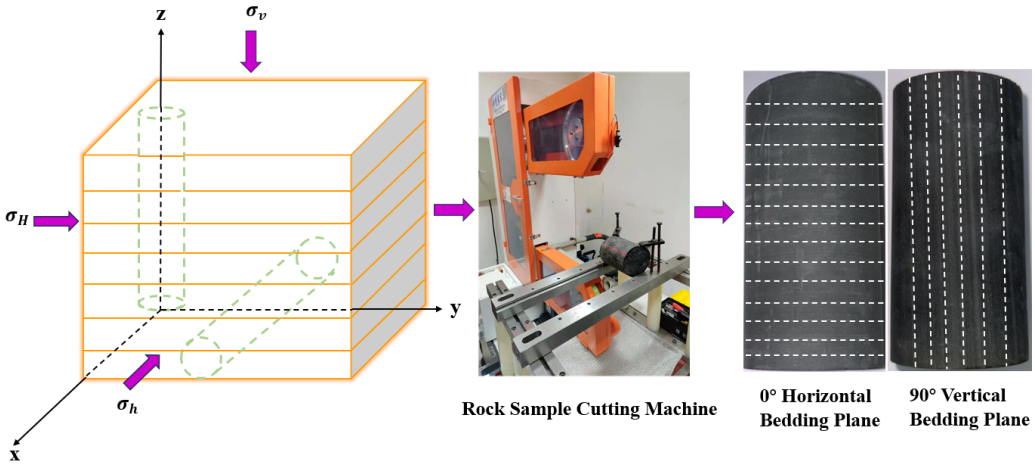


Figure 1. Schematic diagram of oriented core sample preparation.

2.2. Compressive Strength Testing Apparatus

All experiments were conducted using a GCTS RTR-1500 triaxial rock testing system from Tempe, Arizona, USA, which is equipped with high-temperature and high-pressure (HTHP) capabilities. This apparatus has a maximum load capacity of 100 kN (with a relative error of less than ±0.50%) and a strain measurement range of 0.2–100% of full scale (FS), as illustrated in Figure 2. The testing protocol employed axial displacement control, following a two-stage loading sequence: (1) Axial loading at a rate of 10 mm/min until initial contact between the indenter and the specimen was confirmed; (2) Subsequent

loading at a reduced rate of 0.1 mm/min after resetting the displacement baseline to ensure precise strain acquisition.

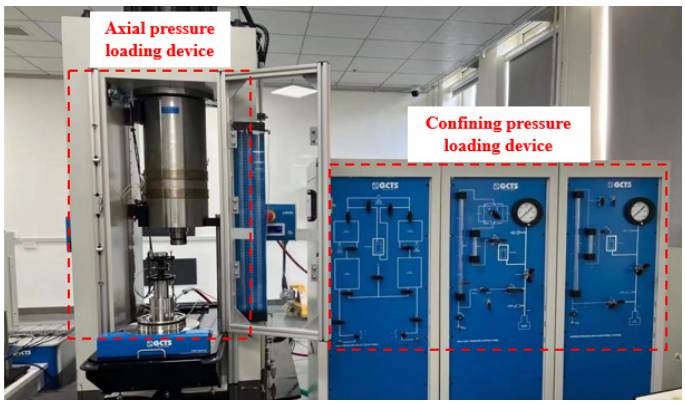


Figure 2. GCTS RTR-1500 high-temperature and high-pressure rock triaxial testing system.

2.3. Compressive Strength Test Results

The triaxial compressive strength results of shale specimens subjected to oil-based drilling fluid invasion are presented in Table 1, while the time-dependent strength evolution is illustrated in Figure 3. The data reveal distinct mechanical responses based on bedding orientations. At a 90° bedding orientation (with the loading direction parallel to the bedding planes), the triaxial compressive strength showed minimal variation as the exposure time to the drilling fluid increased. At a 0° bedding orientation (with the loading direction perpendicular to the bedding planes), a rapid reduction in linear strength occurred within the first 48 h, followed by an accelerated degradation phase (from 48 to 72 h) at a rate of 1.21 MPa per hour. Beyond 72 h, the strength stabilized asymptotically, indicating the presence of a critical weakening threshold. Mechanistic analysis indicates that short-term exposure to oil-based drilling fluid has a minimal impact on the shale matrix. The observed degradation in strength primarily results from fluid invasion along bedding planes, which undermines interlayer cohesion. In the case of a 0° bedding orientation, the orthogonal alignment of the loading direction to the bedding planes reduces bedding-induced anisotropy, leading to minimal time-dependent variations in strength. Conversely, at a 90° bedding orientation, axial loading directly activates the shear strength of the shale matrix, thereby exacerbating the effects of bedding-controlled strength deterioration. Based on these observations, time-dependent strength degradation models for bedded shale subjected to drilling fluid invasion have been established, as formulated in Equations (1) and (2):

$$y1 = 0.0003x^2 - 0.0629x + 77.046 \quad (1)$$

$$y2 = \begin{cases} -0.2281x + 70.885, & 0\text{–}48\ \text{h} \\ -1.2125x + 118.12, & 48\text{–}72\ \text{h} \\ 30, & > 72\ \text{h} \end{cases} \quad (2)$$

where x represents the drilling fluid invasion time, h; y denotes the triaxial compressive strength under 30 MPa confining pressure, MPa.

The analysis of the data presented in Table 2 indicates that shale specimens subjected to a 72 h immersion in drilling fluid retain significant anisotropy in compressive strength when subjected to confining pressure between horizontal (0°) and vertical (90°) bedding orientations. When loaded parallel to the bedding planes (0°orientation), the triaxial compressive strength of specimens immersed in oil-based drilling fluid exhibited a 56.5% reduction compared to baseline values, along with a 5.4% decrease in cohesion. In contrast, specimens loaded perpendicular to the bedding planes (90° orientation) demonstrated

only a 4.1% reduction in strength, with negligible changes in cohesion. Although mechanical degradation occurred in both orientations, the vertical bedding direction exhibited substantially less-pronounced weakening effects, which can be attributed to the inherent heterogeneity of laminated shale formations. This experimental investigation systematically quantifies the mechanical evolution of bedded shale through comparative triaxial testing conducted before and after the invasion of oil-based drilling fluid. The physical characterization focused on two critical orientations: horizontal bedding planes (0° loading) and vertical bedding planes (90° loading). The acquired dataset provides essential parameters for developing constitutive models that describe the interaction mechanisms between drilling fluid and shale, specifically addressing the strength anisotropy induced by fluid invasion in organic-rich laminated shales.

Table 1. Experimental results of triaxial strength following immersion in oil-based drilling fluid.

Drilling Fluid Type	Coring Direction (°)	Well Number	Rock Sample Number	Confining Pressure (MPa)	Soaking Time (h)	Rock Mechanics Parameters		
						Triaxial Compressive Strength (MPa)	Young's Modulus (MPa)	Poisson's Ratio
Oil-Based Drilling Fluid	0	G2	1-1	30	0	70.87	23.44	0.172
		G2	1-2	30	24	66.44	22.89	0.155
		G2	1-3	30	48	59.92	23.15	0.106
		G2	1-4	30	72	30.82	11.72	0.167
		G2	1-5	30	96	30.52	11.68	0.15
		G2	1-6	30	120	30.36	11.56	0.174
	90	G4	2-1	30	0	76.98	20.13	0.178
		G4	2-2	30	24	75.86	20.06	0.143
		G4	2-3	30	48	74.55	19.89	0.157
		G4	2-4	30	72	73.91	15.92	0.138
		G4	2-5	30	96	73.55	13.24	0.159
		G4	2-6	30	120	73.43	13.56	0.145

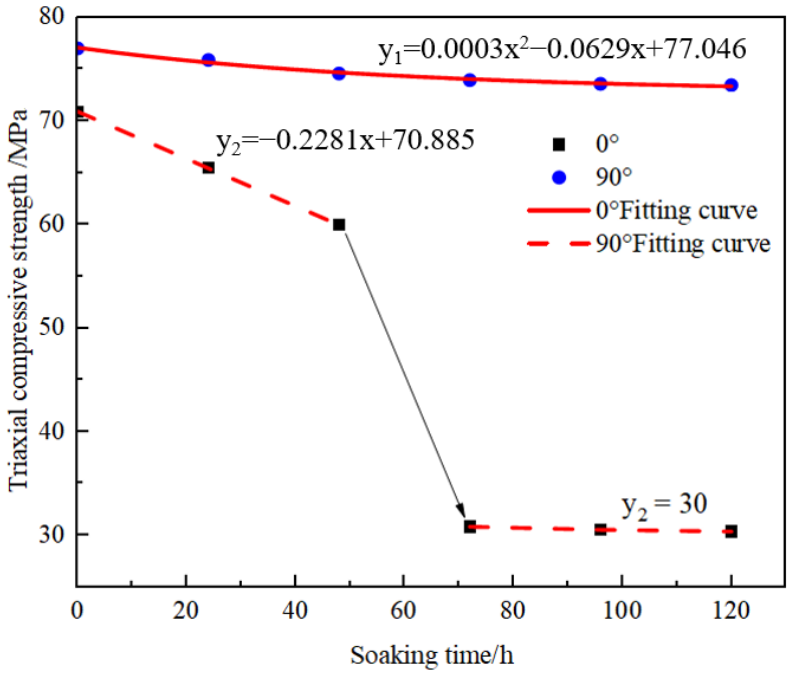


Figure 3. Variation in triaxial strength of core samples after immersion in oil-based drilling fluid.

Table 2. Triaxial mechanical properties of bedded shale before and after drilling fluid immersion.

Coring Direction (°)	Before and After Soaking	Rock Sample Number	Confining Pressure (MPa)	Elastic Modulus (GPa)	Poisson's Ratio	Compressive Strength (MPa)	Cohesion (MPa)	Internal Friction Angle (°)
0	Before Soaking	1-7	0	23.15	0.196	69.34	11.683	13.65
		1-8	15	23.54	0.218	70.65		
		1-1	30	23.44	0.172	70.87		
90	Before Soaking	2-7	0	20.53	0.269	73.71	25.638	15.42
		2-8	15	19.76	0.204	75.18		
		2-1	30	20.13	0.178	76.98		
0	After Soaking	1-9	0	11.57	0.187	30.16	6.225	8.11
		1-10	15	11.79	0.202	30.73		
		1-4	30	11.72	0.167	30.82		
90	After Soaking	2-9	0	15.11	0.159	70.75	25.524	8.78
		2-10	15	10.37	0.171	72.11		
		2-4	30	15.92	0.138	73.91		

3. Strength Criteria for Drilling Fluid Invasion in Bedding Shale

The moisture content of shale serves as a critical indicator for assessing the extent of strength degradation following water absorption. By integrating the enhanced generalized Hoek–Brown anisotropic strength criterion proposed by Saroglou and Tsiambaos, a strength criterion for drilling fluid invasion in bedding shale has been established. The model is founded on the following assumptions: (1) Water molecules that penetrate along the bedding planes of shale will interact with clay minerals, resulting in hydration; (2) The strength degradation of bedding shale is attributed to the hydration of clay minerals and is directly proportional to the moisture content within the shale.

For shale, a type of rock characterized by anisotropy, Saroglou and Tsiambaos [23] introduced a parameter (k_β) based on the Hoek–Brown strength criterion to describe the anisotropic properties of shale. The enhanced generalized Hoek–Brown anisotropic strength criterion is expressed in Equation (3):

$$\sigma_1 = \sigma_3 + \sigma_{c\beta}\left[k_\beta m_i \frac{\sigma_3}{\sigma_{c\beta}} + 1\right]^{0.5} \tag{3}$$

In the equation, β—The angle between the shale bedding plane and the axial loading stress, measured in degrees (°); $\sigma_{c\beta}$—The uniaxial compressive strength when the angle between the shale bedding plane and the axial loading stress is β, expressed in megapascals (MPa); k_β—A parameter related to the angle β between the shale bedding plane and the axial loading stress, If the axial loading stress is perpendicular to the shale bedding plane, $k_{90} = 1$; If the axial loading stress is parallel to the shale bedding surface, $k_0 = 0.8$; m_i—Parameters determined based on the mineral composition of shale, $m_i = 12$.

This strength criterion for hydrated bedding shale defines a shale hydration degree ratio ψ:

$$\begin{cases} \psi = \frac{\omega}{\zeta\eta} \\ \eta = \frac{M_w - M_d}{\zeta M_d} \end{cases} \tag{4}$$

In the equation, ω—Moisture content of shale, %; ζ—Clay mineral content, %; η—Water absorption coefficient of clay, defined as the ratio of the mass of water absorbed by saturated shale to the mass of dried clay minerals in the shale; M_w—Mass of saturated shale, g; M_d—Mass of dried shale, g.

After absorbing water from drilling fluid or formation fluids, shale undergoes hydration and expansion. This expansion stress can be regarded as an equivalent pore pressure. Under different confining pressures and angles between the axial loading stress and the

bedding plane, the linear correlation coefficient between the uniaxial compressive strength of shale and its moisture content is above 0.8, indicating a strong linear relationship between the uniaxial compressive strength and moisture content. Therefore, the water absorption expansion stress (σ_{wF}) at the peak uniaxial compressive strength can be expressed by Equation (5).

$$\sigma_{wF} = F\psi = F\frac{\omega}{\zeta\eta} \tag{5}$$

In the equation, σ_{wF} represents the equivalent pore pressure of shale hydration swelling stress under a stress-free state, MPa; F is the equivalent pore pressure coefficient of shale hydration under a stress-free state.

For the case where shale is subjected to uniaxial stress only, the equivalent pore pressure can be regarded as a reduction in the uniaxial compressive strength relative to the dried shale. Therefore, under uniaxial stress conditions, the strength of hydrated laminated shale ($\sigma_{cw\beta}$) can be expressed by Equation (6) as follows:

$$\sigma_{cw\beta} = \sigma_{c\beta} - \sigma_{wF} = \sigma_{c\beta} - F\frac{\omega}{\zeta\eta} \tag{6}$$

Substituting Equations (4) and (5) into Equation (6), we subsequently derive Equation (7):

$$\sigma_{cw\beta} = \sigma_{c\beta} - \frac{F\omega M_d}{M_w - M_d} \tag{7}$$

By combining Equations (3) and (7), we establish the strength failure criterion for hydrated laminated shale under triaxial stress conditions:

$$\begin{aligned} \sigma_1 &= \sigma_3 + \sigma_{cw\beta}\left[k_\beta m_i \frac{\sigma_3}{\sigma_{cw\beta}} + 1\right]^{0.5} \\ &= \sigma_3 + \left(\sigma_{c\beta} - \frac{F\omega M_d}{M_w - M_d}\right)\left[\frac{k_\beta m_i \sigma_3 (M_w - M_d)}{\sigma_{c\beta}(M_w - M_d) - F\omega M_d} + 1\right]^{0.5} \end{aligned} \tag{8}$$

4. Numerical Simulation Study on the Strength Degradation of Bedding Shale Due to Drilling Fluid Invasion

4.1. Establishment and Validation of the Numerical Model

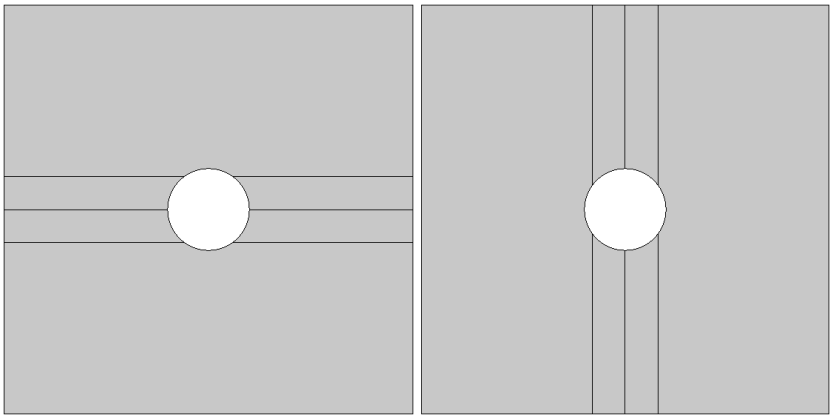
To verify the accuracy of the mathematical model established in this study, a drilling fluid invasion model was developed based on the interfaces of Darcy flow and fracture flow models. The finite element method was systematically employed to investigate the invasion patterns of drilling fluid in shale. As illustrated in Figure 4a, the horizontal bedding plane at 0° is depicted, while Figure 4b shows the vertical bedding plane at 90° in a horizontal well. Utilizing the shale formation parameters listed in Table 3, the effects of invasion pressure, the number of bedding planes, and bedding aperture on the strength degradation of shale in the 0° and 90° bedding directions were analyzed.

Table 3. Basic parameters of shale formation.

Parameter	Value	Unit
Shale Elastic Modulus	25	GPa
Shale Poisson's Ratio	0.25	/
Shale Density	2500	kg/m^3
Shale Matrix Porosity	3	%
Shale Matrix Permeability	1×10^{-20}	m^2
Shale Bedding-Plane Porosity	15	%
Shale Bedding-Plane Permeability	1×10^{-9}	m^2

Table 3. *Cont.*

Parameter	Value	Unit
Oil-Based Drilling Fluid Density	1800	kg/m^3
Intrusion Pressure	6, 7, 8	MPa
Number of Shale Bedding Planes	3, 5, 9	Line
Shale Bedding-Plane Aperture	1×10^{-6}, 1×10^{-4}, 1×10^{-3}	m



(**a**) 0° Horizontal Bedding Plane (**b**) 90° Vertical Bedding Plane

Figure 4. Establishment of the numerical model.

Figure 5 illustrates the comparison between the simulation results and the experimental measurement data. The horizontal axis represents the distance from the well axis, while the vertical axis indicates saturation levels. The comparison presented in Figure 5 demonstrates that the simulation results closely align with the experimental data, suggesting that the mathematical model effectively predicts changes in saturation during the experiment. This alignment validates the model's accuracy and effectiveness.

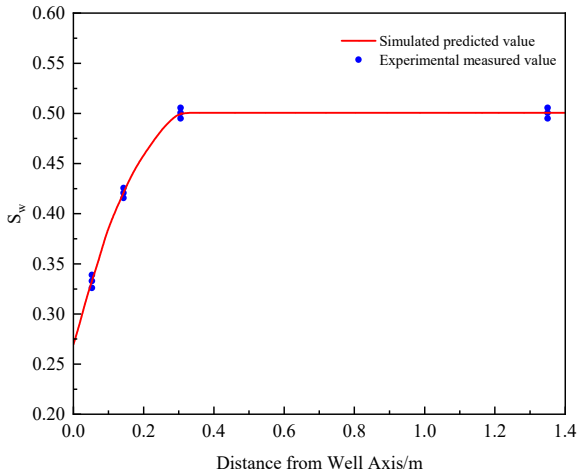


Figure 5. Verification of simulation and experimental results.

It is important to clarify that the model is based on Darcy's law, which applies to laminar flow (Reynolds number Re < 10), as well as the fracture flow equation. The underlying premise is that fluid flow is predominantly influenced by viscous forces (i.e., Re $\ll$ 1). For Newtonian fluids, the Reynolds number is defined as follows:

$$\mathrm{Re} = \frac{\rho v D_h}{\mu} \tag{9}$$

In the formula, ρ represents the density of the drilling fluid, kg/m^3; v denotes the Darcy flow velocity, m/s; D_h indicates the hydraulic diameter of the bedding fracture, m; μ signifies the dynamic viscosity, Pa·s.

When the Reynolds number (Re) exceeds 10, inertial forces increase, resulting in a transition to turbulent flow and invalidating the linear assumption of Darcy's law. In the simulations conducted in this study, as detailed in the parameters outlined in Table 3, the matrix permeability is extremely low, measuring 10^{-20} m^2. The maximum Reynolds number of approximately 8 in the crack corresponds to an opening of 10^{-3} m, which remains within the laminar flow regime. For scenarios involving higher flow velocities or wider cracks (Re > 30), the Forchheimer equation or a turbulence correction model should be employed.

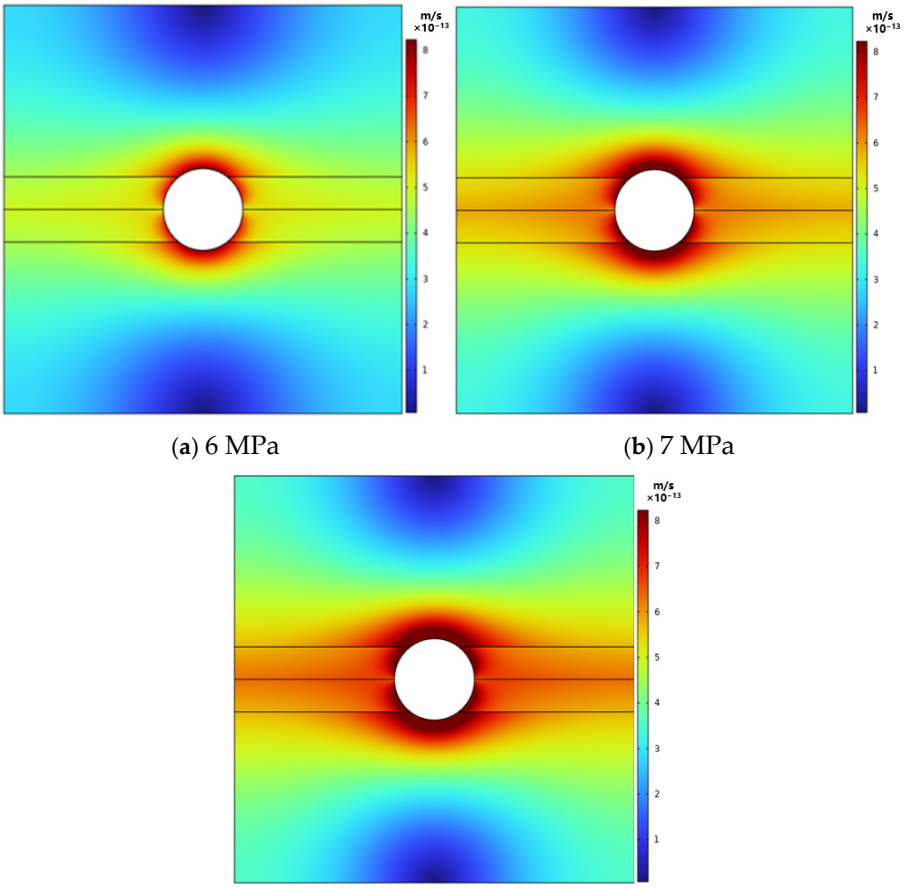
4.2. Fluid Permeability Characteristics in the 0° and 90° Bedding Directions Under Varying Invasion Pressures

The invasion of drilling fluid into shale can lead to the accumulation of pore pressure, thereby weakening the mechanical strength of the shale. Intrusion pressure is a critical control parameter for the permeability of drilling fluid. Variations in intrusion pressure directly influence the depth of drilling fluid penetration and the distribution of pore pressure, resulting in differing degrees of strength degradation in the shale. There are significant differences in the permeability behavior and mechanical property degradation of shale when subjected to bedding directions of 0° (parallel to the bedding direction) and 90° (perpendicular to the bedding direction). In cases where the shale bedding consists of three layers and the bedding opening measures 1×10^{-4} m, numerical simulation analysis is performed to investigate the impact of drilling fluid invasion on shale strength degradation under various invasion pressures (6 MPa, 7 MPa, and 8 MPa), thereby elucidating the underlying mechanisms and patterns.

In the horizontal bedding direction at 0°, as the invasion pressure increases from 6 MPa to 8 MPa, the phenomenon of drilling fluid invasion becomes increasingly pronounced. Figure 6 illustrates that at a low invasion pressure of 6 MPa, the fluid flow near the wellbore is relatively gentle, and the velocity distribution is fairly uniform, with only slight increases in flow observed in localized areas. When the pressure rises to 7 MPa, the fluid flow velocity around the wellbore, particularly at the intersections of bedding planes, significantly increases, resulting in an area of elevated velocity that exhibits outward diffusion. At 8 MPa, a substantial high-speed invasion zone forms around the wellbore, accompanied by an increase in peak velocity. The drilling fluid aggressively invades along the horizontal bedding direction, intensifying the disturbance to the shale structure. This indicates that as the invasion pressure escalates, the drilling fluid is more likely to overcome the resistance of shale pores and throats, rapidly infiltrating along the horizontal bedding and exacerbating the deterioration of shale strength. Consequently, the originally stable internal structure of the shale gradually loosens and weakens under the impact of the fluid.

For the 90° vertical bedding direction, variations in invasion pressure lead to distinct invasion phenomena. As illustrated in Figure 7, when the invasion pressure is set at 6 MPa, the fluid flow at the wellbore is only slightly active; however, the overall invasion depth remains shallow, and the velocity does not exhibit significant changes, primarily concentrating within a narrow range near the wellbore. As the pressure increases to 7 MPa, the penetration force of the fluid in the vertical bedding direction intensifies, resulting in a deeper invasion depth. Additionally, the area of increased velocity extends both upward and downward along the bedding, creating more pronounced longitudinal invasion channels. When the pressure reaches 8 MPa and the fluid invades at high speed, a significant high-speed invasion zone forms above and below the wellbore, greatly expanding the invasion range. The drilling fluid rapidly surges and sinks along the vertical bedding,

exerting a strong impact on the shale and disrupting the interlayer bonding forces, which leads to a substantial decrease in shale strength. Furthermore, this vertical invasion can easily induce instability in the wellbore wall, further compromising the safety of drilling operations and the integrity of the shale.

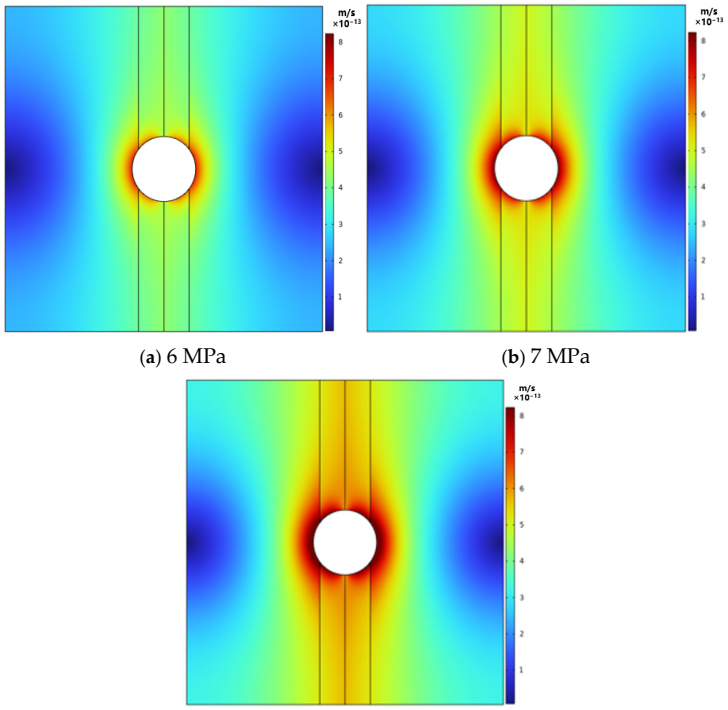


(**a**) 6 MPa (**b**) 7 MPa

(**c**) 8 MPa

Figure 6. 0° bedding plane.

In contrast, when the invasion pressure remains constant, the drilling fluid invasion in the 0° horizontal bedding direction primarily focuses on diffusion across the horizontal plane. The fluid extends horizontally along the bedding plane, thereby expanding the invasion area and gradually eroding the horizontal bedding structure of the shale, which results in a deterioration of strength uniformity. Conversely, the 90° vertical bedding direction is characterized by intensified vertical depth invasion, where fluids tend to penetrate rapidly both upward and downward along the vertical bedding. This can cause significant damage to the interlayer stability of the shale in the vertical direction, leading to a sharp decrease in local strength and even posing a risk of wellbore collapse. From the perspective of invasion pathways, horizontal bedding facilitates the lateral movement of fluids, resulting in a broad yet relatively gentle impact range. In contrast, vertical bedding creates a channel for the vertical penetration of fluids, which exerts concentrated destructive forces. The extent of damage is likely to become more pronounced with increasing pressure. There are significant differences between the two bedding orientations regarding their invasion modes and their effects on the degradation of shale strength. Therefore, it is essential to accurately prevent and control the risk of drilling fluid invasion during actual drilling operations, taking into account the orientation of the bedding.



(**a**) 6 MPa (**b**) 7 MPa

(**c**) 8 MPa

Figure 7. 90° bedding plane.

Figure 8 illustrates the distribution of water saturation after three days of invasion by oil-based drilling fluid at invasion pressures of 6 MPa, 7 MPa, and 8 MPa, respectively. The radial profiles of saturation indicate that at lower invasion pressures, the depth of filtrate invasion is primarily influenced by the invasion pressure. As the invasion pressure increases, the depth of invasion rapidly deepens. However, as the invasion pressure continues to rise, the combined limiting effects of formation permeability, pore compression, capillary forces, and filter cake formation become increasingly evident, impeding further filtrate invasion and ultimately leading to the stabilization of the invasion depth. This results in the formation reaching a dynamic equilibrium state regarding filtrate invasion. This process highlights the dynamic equilibrium mechanism that involves the interplay of multiple factors during filtrate invasion.

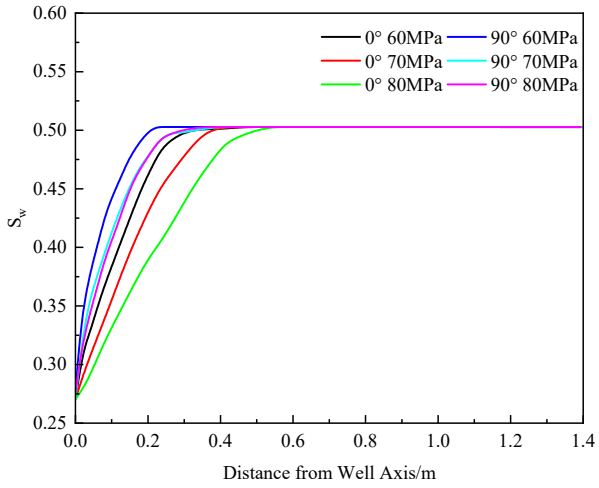
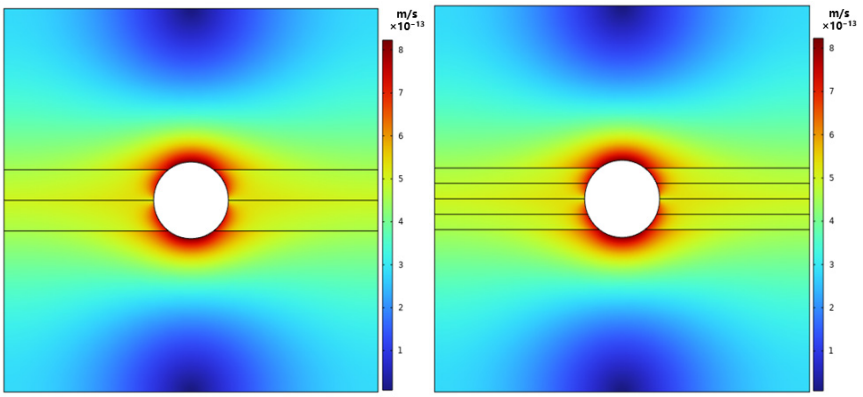


Figure 8. Variation characteristics of water saturation under different invasion pressures of oil-based drilling fluids.

4.3. Fluid Permeability Characteristics in the 0° and 90° Bedding Directions Under Varying Numbers of Bedding Planes

Shale exhibits a significant degradation of mechanical properties under conditions of drilling fluid invasion. The intrusion of drilling fluid can result in increased pore pressure within the shale and structural weakening, particularly in shales with complex bedding structures, where the degradation effect is more pronounced. When the invasion pressure is 6 MPa and the shale bedding opening is 1×10^{-4} m, the strength degradation behavior of shale at bedding direction angles of 0° and 90° is investigated through numerical simulation methods. This study explores the effects of varying bedding numbers (three, five, and nine layers) during drilling fluid invasion, revealing the underlying mechanisms and patterns of degradation.

In the direction of the 0° horizontal bedding plane, as the number of bedding planes increases from three to nine, the phenomenon of drilling fluid invasion gradually intensifies. As illustrated in Figure 9, when the number of layers is three, the fluid flow around the wellbore is relatively gentle, the invasion range is narrow, and the invasion velocity is low, primarily concentrated in the vicinity of the wellbore. When the number of layers increases to five, the invasion range expands, the fluid flow velocity significantly increases, and the invasion depth deepens, particularly at the intersections of layers where distinct invasion channels form. When the number of layers reaches nine, a large-scale, high-speed intrusion zone emerges around the wellbore, characterized by a substantial increase in peak intrusion velocity and further expansion of both intrusion depth and range. This indicates that as the number of bedding planes increases, drilling fluid is more likely to diffuse in the horizontal bedding direction, thereby increasing the disturbance to the shale structure and exacerbating the degradation of shale strength.

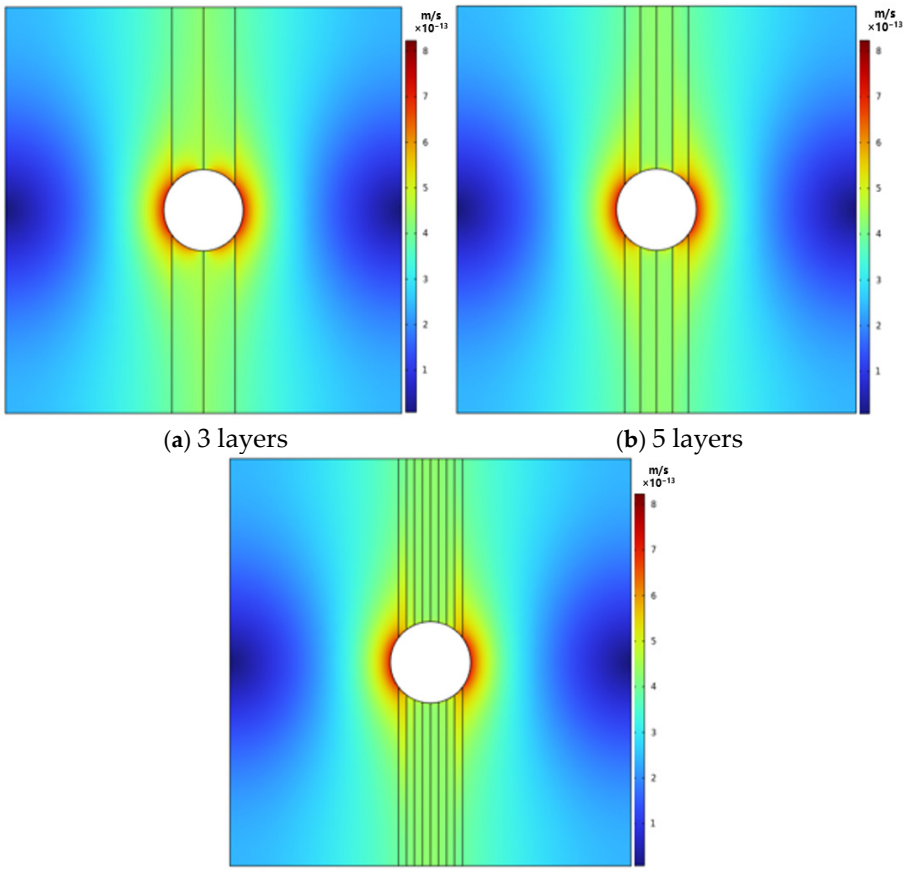


(**a**) 3 layers (**b**) 5 layers

(**c**) 9 layers

Figure 9. 0° bedding plane.

From Figure 10, it is evident that in the 90° vertical bedding direction, the fluid diffuses outward from the wellbore, with the velocity field gradually decreasing radially. This transition occurs from high-velocity areas (red) to low-velocity areas (yellow and orange), demonstrating a relatively symmetrical distribution. The bedding fracture zone is represented as a low-velocity region (blue area), which significantly restricts the longitudinal flow of the fluid. Within the bedding fracture, the fluid flow velocity is low, causing the fluid to diffuse primarily along the matrix area. The flow is notably influenced by the bedding structure. Cracks manifest as regions of reduced flow velocity within the overall velocity field, indicating their obstructive effect on fluid movement. Fluid diffusion predominantly occurs along the highly permeable areas of the matrix, and the number of layers has a relatively minor impact on strength.



(**a**) 3 layers (**b**) 5 layers

(**c**) 9 layers

Figure 10. 90° bedding plane.

The permeability of bedding fractures demonstrates significant anisotropy, exhibiting higher permeability in the direction parallel to the fractures and lower permeability in the vertical direction. As the number of bedding planes increases, the bedding structure alters the diffusion path of the drilling fluid considerably. When the bedding plane is horizontal at 0°, a greater number of bedding planes results in a more concentrated seepage path along the bedding plane, thereby enhancing the anisotropy of the Darcy velocity distribution. Conversely, when the bedding plane is oriented perpendicularly at 90°, the barrier effect of the bedding plane on the drilling fluid becomes more pronounced, significantly restricting the seepage path.

Figure 11 illustrates the distribution of water saturation after three days of invasion by oil-based drilling fluid under conditions with three, five, and nine bedding layers, respectively. The radial profiles of saturation indicate that as the number of bedding layers

increases, the invasion depth of the drilling fluid filtrate initially exhibits significant growth. This phenomenon is primarily attributed to the additional seepage channels created by the increased number of bedding interfaces, which greatly enhance the diffusion of the filtrate. However, as the number of bedding layers continues to rise, the overall permeability of the formation tends to reach a saturation point. Concurrently, limiting factors such as capillary forces, formation heterogeneity, and filter cake effects gradually become more pronounced, ultimately causing the invasion depth to stabilize. This trend highlights the complex dynamic equilibrium mechanisms involved in the filtrate invasion process within multi-bedding formations.

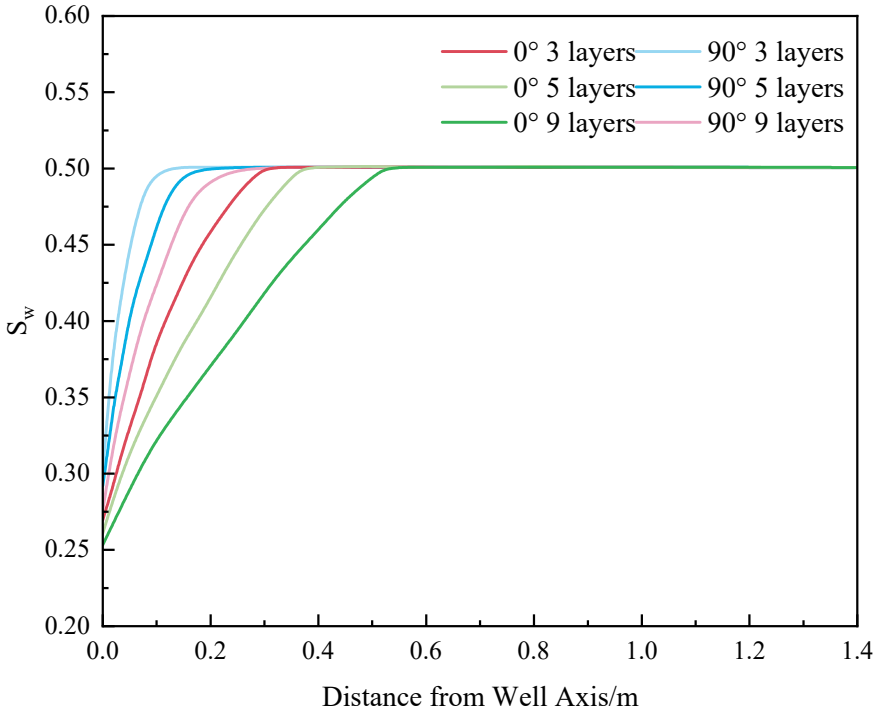


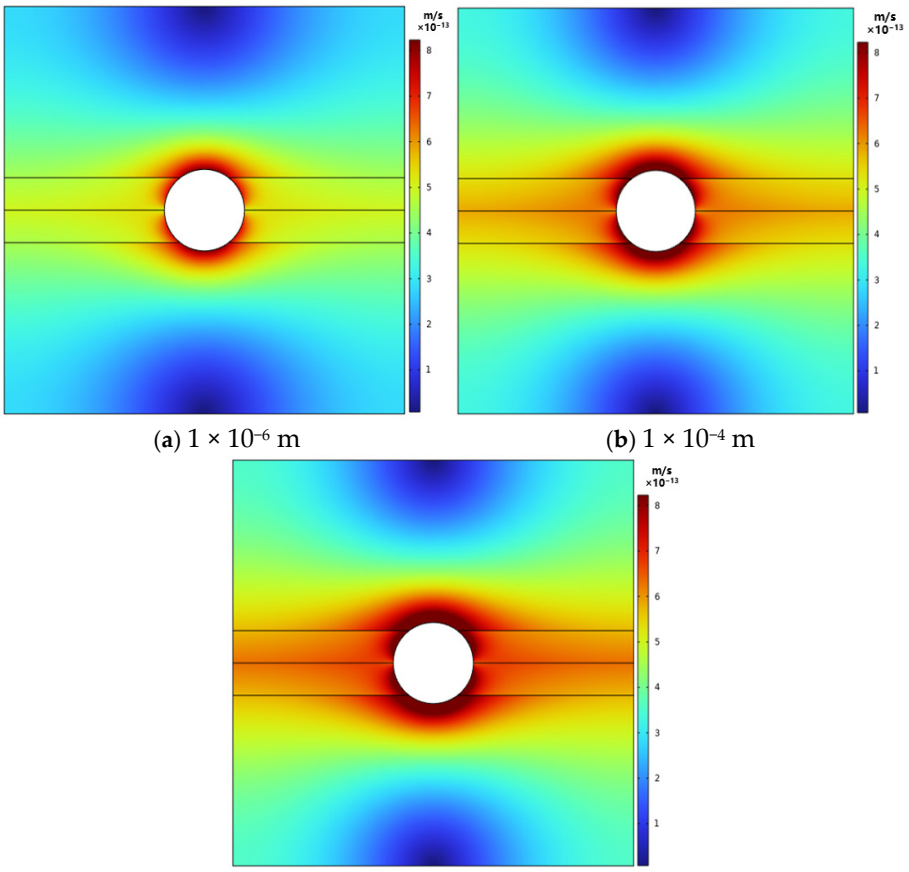
Figure 11. Variation characteristics of water saturation under different bedding configurations of oil-based drilling fluid.

4.4. Fluid Permeability Characteristics in the 0° and 90° Bedding Directions Under Varying Degrees of Bedding-Plane Opening

After drilling fluid invades shale, it causes changes in shale strength, particularly in the presence of bedding fractures. The degree of bedding opening significantly influences the degradation process of shale strength. There is a notable difference in the mechanical behavior of shale when the bedding direction angle is 0° compared to 90°. When the invasion pressure is 6 MPa and the number of shale layers is three, the impact of drilling fluid invasion on shale strength degradation was analyzed through numerical simulation, considering different layer opening degrees (1×10^{-6} m, 1×10^{-4} m, and 1×10^{-3} m).

In the horizontal bedding direction at 0°, as the bedding opening increases from 1×10^{-6} m to 1×10^{-3} m, the phenomenon of drilling fluid invasion significantly intensifies. As illustrated in Figure 12, when the bedding opening is 1×10^{-6} m, the distribution of Darcy velocity is relatively uniform, with the velocity field primarily concentrated around the walls of the drilling hole. The guiding effect of cracks on fluid movement is weak, resulting in the fluid mainly diffusing radially without establishing a clear preferential permeation path. The influence of the bedding interface is relatively minor, and cracks do not significantly increase the Darcy velocity. The degree of strength degradation in shale is relatively low, with the primary manifestation of cracks being a reduction in bonding strength, accompanied by localized shear slip. When the opening degree of the bedding

plane is 1×10^{-4} m, the area with high Darcy velocity begins to distribute along the horizontal bedding direction, indicating that the cracks preferentially guide fluid diffusion. The seepage capacity at the bedding cracks is enhanced, resulting in more pronounced horizontal diffusion channels. Pore pressure is significantly concentrated around the cracks, and the velocity distribution exhibits a degree of anisotropy. The material strength deteriorates considerably, leading to crack propagation and penetration along the bedding plane, with the primary failure mode being interlayer slip. When the opening degree of the bedding plane is 1×10^{-3} m, the Darcy velocity distribution exhibits a distinct horizontal band-like extension, with high-value areas concentrated entirely at the cracks in the bedding plane. These cracks create significant preferential infiltration pathways, allowing fluid to flow predominantly along the horizontal cracks, while radial seepage is primarily influenced by these cracks. The range of high Darcy velocities is broad and evenly distributed, indicating that the impact of bedding cracks is at its peak. The strength of the shale decreases sharply, leading to interlayer slip and interface delamination that penetrates the entire model. This results in a failure mode characterized by interlayer instability.

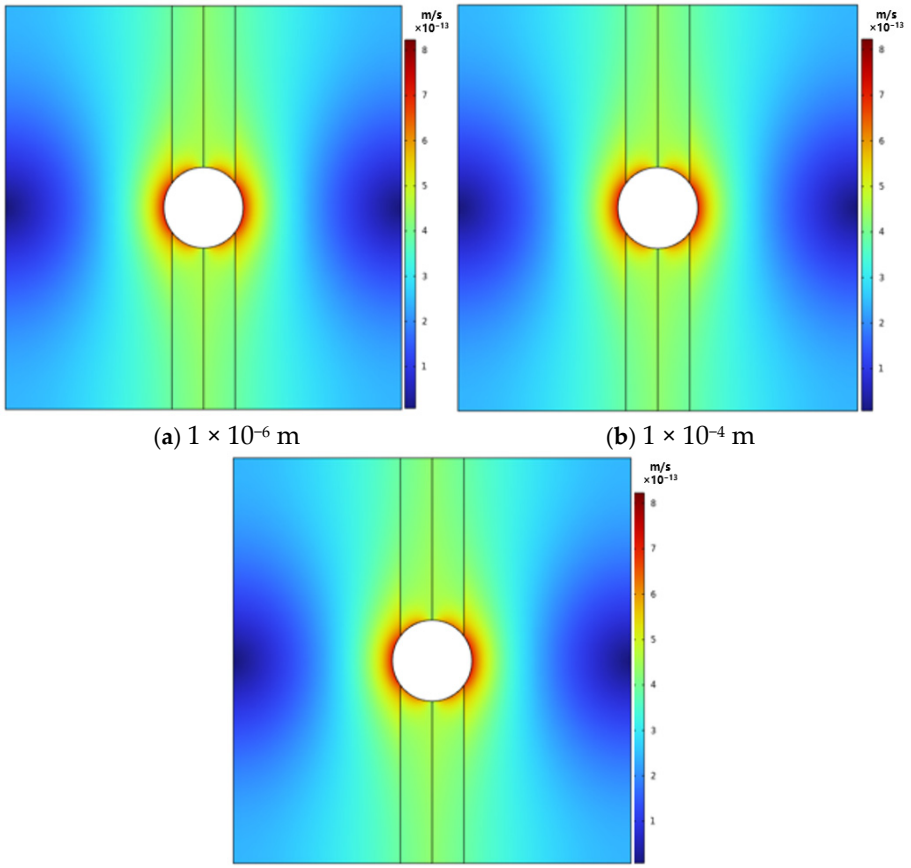


(**a**) 1×10^{-6} m (**b**) 1×10^{-4} m

(**c**) 1×10^{-3} m

Figure 12. 0° bedding plane.

From Figure 13, it is evident that changes in bedding openings have a relatively minor effect on the invasion phenomenon in the 90° vertical bedding direction. Regardless of whether the layer opening is 1×10^{-6} m, 1×10^{-4} m, or 1×10^{-3} m, fluid flow at the wellbore remains relatively active; however, the invasion depth is relatively shallow. The invasion range is primarily concentrated around the wellbore, with minimal variation in invasion velocity. This suggests that increasing the bedding opening in the vertical direction has a limited impact on drilling fluid invasion, and the degradation of shale strength is relatively mild.



(**a**) 1 × 10⁻⁶ m (**b**) 1 × 10⁻⁴ m

(**c**) 1 × 10⁻³ m

Figure 13. 90° bedding plane.

In the direction of the 0° horizontal bedding plane, an increase in bedding-plane opening significantly enhances the invasion of drilling fluid. Both the speed and range of this invasion increase markedly with the degree of opening, leading to a severe deterioration of shale strength and potentially causing wellbore instability. Conversely, in the 90° vertical bedding direction, although the bedding opening increases, the intrusion phenomenon remains relatively unchanged, resulting in a smaller intrusion depth and range, which has a limited impact on the degradation of shale strength. This suggests that the horizontal bedding direction is more sensitive to the degree of bedding opening, making it more likely for drilling fluid to diffuse along the horizontal bedding and damage the shale structure. In contrast, the intrusion channels in the vertical bedding direction are relatively restricted, and the influence of bedding opening is not significant. Therefore, during actual drilling operations, it is crucial to monitor the risk of drilling fluid invasion in the horizontal bedding direction to effectively maintain wellbore stability and preserve shale strength.

Figure 14 illustrates the distribution of water saturation after three days of invasion by oil-based drilling fluid through bedding apertures of 1×10^{-6} m, 1×10^{-4} m, and 1×10^{-3} m, respectively. The radial profiles of saturation indicate that the invasion depth of the drilling fluid filtrate initially increases rapidly as the bedding aperture enlarges. This phenomenon is primarily attributed to the significant enhancement of formation permeability and the reduction of capillary pressure resulting from the increased bedding aperture, which decreases the resistance to filtrate invasion. However, when the aperture exceeds a certain critical value, the formation permeability tends to reach a saturation point, and the influence of capillary pressure diminishes to a negligible level. At this stage, the combined effects of filter cake formation and the inherent permeability of the formation restrict the further expansion of the filtrate, causing the invasion depth to

gradually stabilize. This dynamic process reflects the characteristic equilibrium among multiple physical mechanisms during filtrate invasion.

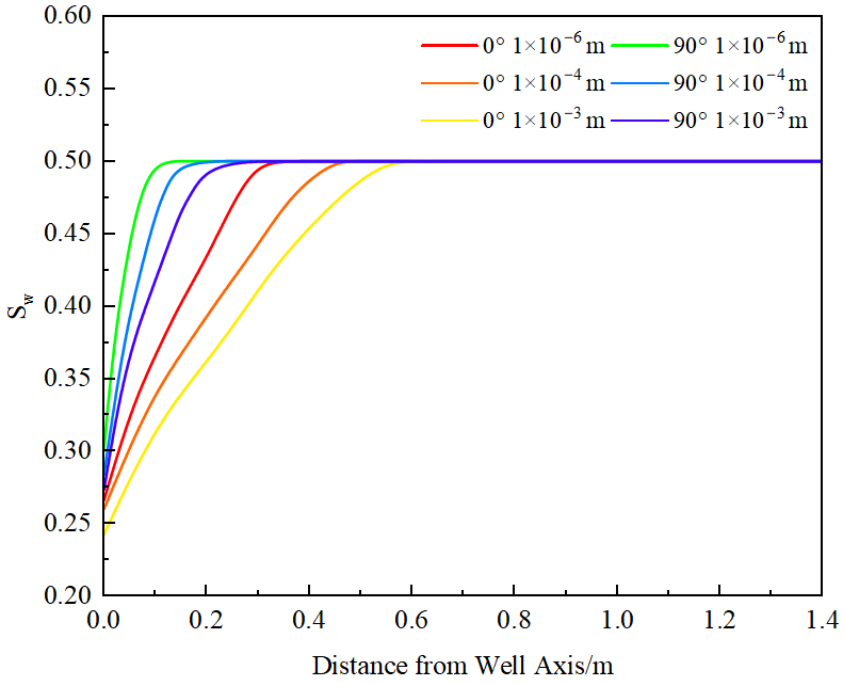


Figure 14. Variation characteristics of water saturation at different bedding opening degrees of oil-based drilling fluid.

4.5. Flow Characteristics of Drilling Fluids: Flow States and Model Applicability

The drilling fluid discussed in this article is classified as a Newtonian fluid (μ = 0.022 Pa·s); however, oil-based drilling fluids often exhibit non-Newtonian characteristics, particularly shear-thinning behavior. For non-Newtonian fluids, the generalized Reynolds number (Re_M) should be employed.

$$Re_M = \frac{\rho v^{2-n} D_h^n}{K\left(\frac{3n+1}{4n}\right)^n 8^{n-1}} \tag{10}$$

In the formula, K represents the viscosity coefficient, Pa·s^n), while n denotes the flowability index. When $n = 1$, the equation simplifies to the Newtonian fluid formula (Equation (9)). If $Re_M > 2100$, the flow transitions into the turbulent zone; however, since the flow velocity in shale fractures is typically low (v < 0.05 m/s), Re_M predominantly remains within the laminar range.

When the crack opening exceeds 10^{-3} m or the intrusion pressure surpasses 10 MPa, the local Reynolds number (Re) may exceed 30. At this stage, the influence of inertial forces becomes significant, leading to nonlinear behavior in both the pressure gradient and flow velocity. In such instances, the Forchheimer model should be employed.

$$-\nabla P = \frac{\mu}{k} v + \beta \rho v^2 \tag{11}$$

In the formula, β represents the inertia drag coefficient, m^{-1}. Neglecting this effect may lead to a prediction deviation of more than 15% for high-flow pore pressure.

5. Field Applications

The study of drilling fluid invasion into bedding shale is not only theoretically significant but also offers considerable practical value in drilling engineering. Due to its unique layered structure and complex mechanical properties, bedding shale is particularly vulnerable to the effects of drilling fluid invasion, which can substantially impact wellbore stability and the efficiency of drilling operations. By optimizing the formulation of drilling fluid—specifically by adjusting its viscosity, density, and chemical composition—the invasion of drilling fluid into shale can be mitigated. This reduction minimizes alterations in shale strength and helps prevent wellbore collapse and other potential accidents.

In laboratory studies, key additives such as emulsifiers, organoclay, fluid loss reducers, and sealing agents were selected and optimized through orthogonal experiments to determine their optimal dosages. This process led to the development of a high-performance oil-based drilling fluid system characterized by strong sealing capabilities and low viscosity-high shear properties. The system exhibits the following properties: Rheological properties: $\varphi 6 > 6$, YP/PV > 0.3; Electrical stability: >600 V; Filtration performance: HTHP fluid loss at 120 °C < 2 mL; Settling stability: 1.75 g/cm^3, $\Delta\rho < 0.02$ after 24 h. Furthermore, to evaluate the system's stability, laboratory tests were conducted using a 20% brine solution and 20% low-density solid contamination, which demonstrated excellent resistance to contamination. The system's resilience to water contamination was assessed by incorporating varying amounts of brine (40% calcium chloride solution) into the drilling fluid, which had a density of 1.75 g/cm^3, thereby simulating formation water contamination. Even with a 20% brine addition, the rheological and electrical stability of the drilling fluid remained within acceptable limits, as illustrated in Figure 15. Additionally, the effects of shale cuttings (140 mesh) and British evaluation clay (1:1) on the performance of the drilling fluid were investigated. At a contamination level of 20%, the rheological properties remained stable, as depicted in Figure 16.

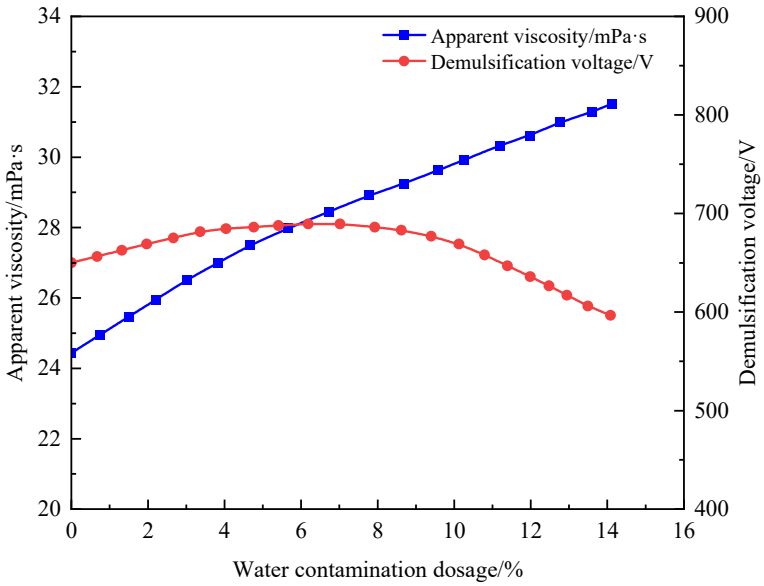


Figure 15. Effect of water addition on system viscosity and demulsification voltage.

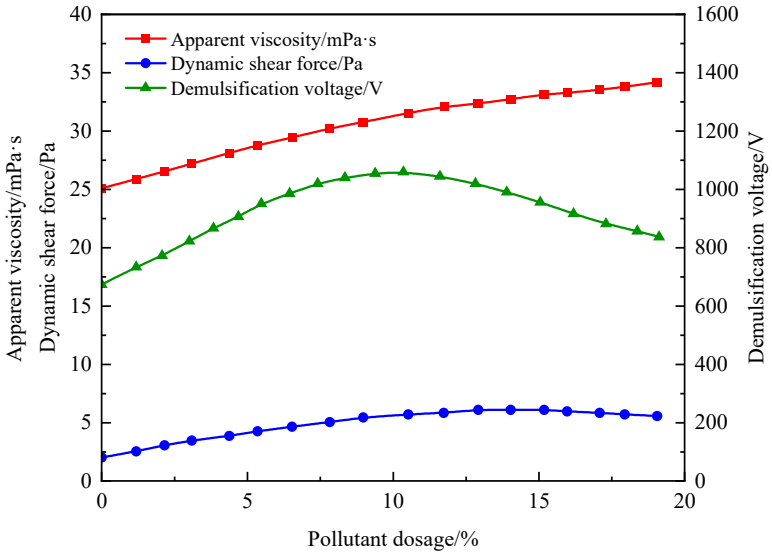


Figure 16. Effect of pollutant dosage on system viscosity and demulsification voltage.

6. Conclusions

(1) The horizontal bedding orientation at 0° indicates that the invasion of drilling fluid along fractures results in a significant reduction in strength. After a soaking period of 72 h, the compressive strength decreases by 56.5%, demonstrating a degradation rate that exceeds 40%. In contrast, the vertical bedding orientation at 90° reveals that permeability is constrained by anisotropy and crack blockage, leading to only a slight reduction in strength of 4.1%.

(2) When the intrusion pressure increases from 6 MPa to 8 MPa, the penetration depth of the horizontal bedding significantly increases, and cracks become the predominant mode of flow. The increase in bedding opening (greater than 10^{-4} m) considerably exacerbates the degradation of strength in the horizontal bedding direction.

(3) The initial development of a quantitative model for Reynolds number degradation indicates that when the Reynolds number exceeds the critical threshold (Re > 10), the transition to turbulence significantly accelerates crack propagation. Furthermore, we propose the Darcy–Forchheimer partitioning algorithm to address the issue of prediction bias exceeding 15% in regions with high Reynolds numbers (Re > 30).

(4) By optimizing the dosage of emulsifiers and other treatment agents through orthogonal experiments, a low-viscosity, high-shear-strength plugging oil-based drilling fluid has been developed. Field applications have demonstrated that this system exhibits strong anti-pollution capabilities, maintaining stable performance even in the presence of 20% saltwater and solid-phase contamination. Furthermore, the depth of drilling fluid invasion has been reduced by more than 30%.

Author Contributions: Writing—original draft preparation, G.W.; Methodology, F.L. and Y.S.; Software, C.K.; Formal analysis, X.W. and L.Z. All authors have read and agreed to the published version of the manuscript.

Funding: The work presented in this paper was financially supported by the First-Class Discipline Collaborative Innovation Program of Heilongjiang Province (Grant No. LJGXCG2024-F02), the Key Research and Development Program of Heilongjiang Province (Grant No. 2024ZX09C01). The Postdoctoral Special Funding of Heilongjiang Province (LBH-TZ2301) is also gratefully acknowledged.

Informed Consent Statement: All authors agreed with the content and that all gave explicit consent to submit and that they obtained consent from the responsible authorities at the institute/organization where the work has been carried out, before the work is submitted.

Data Availability Statement: The data used to support the findings of this study are all shown in uploaded manuscript.

Conflicts of Interest: Guiquan Wang, Yu Suo and Cuilong Kong were employed by the company Daqing Oilfield Co., Ltd. Xiaoguang Wang and Lingzhi Zhou were employed by the Daqing Oilfield Downhole Services Company. The remaining authors declare that the research was conducted in the absence of any commercial or financial relationships that could be construed as potential conflicts of interest.

References

1. Liang, K. Study on Mechanism of Wellbore Collapse and Instability in Horizontal Well of Layered Shale. Master's Thesis, Northeast Petroleum University, Daqing, China, 2023.
2. Zheng, D.; Ozbayoglu, E.; Miska, S.; Zhang, J. Experimental study of anisotropic strength properties of shale. In Proceedings of the ARMA US Rock Mechanics/Geomechanics Symposium, Atlanta, GA, USA, 25–28 June 2023; p. ARMA-2023-0128.
3. Lee, H.; Ong, S.; Azeemuddin, M.; Goodman, H. A wellbore stability model for formations with anisotropic rock strengths. *J. Pet. Sci. Eng.* **2012**, *96*, 109–119. [CrossRef]
4. Zhang, J. Borehole stability analysis accounting for anisotropies in drilling to weak bedding planes. *Int. J. Rock Mech. Min. Sci.* **2013**, *60*, 160–170. [CrossRef]
5. Ahmed, A.A.; Hayfaa, L.S.; Nuhad, A.; Erfan, M.A.L.; Ahmed, I.A.; Swadi, M.; Tariq, K.K. Investigation of the rock strength anisotropy on the wellbore stability analysis. In Proceedings of the ARMA US Rock Mechanics/Geomechanics Symposium, New York, NY, USA, 23–26 June 2019; p. ARMA-2019-0137.
6. Asaka, M.; Holt, R.M. Anisotropic wellbore stability analysis: Impact on failure prediction. *Rock Mech. Rock Eng.* **2021**, *54*, 583–605. [CrossRef]
7. Ma, T.S.; Tang, T.; Chen, P.; Chen, C.; Sun, S.L.; Liu, Y.Y. Prediction of borehole fracture pressure in anisotropic formations. *J. China Univ. Pet. Nat. Sci. Ed.* **2019**, *43*, 80–89.
8. Li, Z.T.; Zhang, Z.; Wu, P.C.; Ma, T.S.; Fu, J.H. Mechanical mechanism of wellbore instability in deep anisotropic shale in southern Sichuan. *J. Southwest Pet. Univ. Nat. Sci. Ed.* **2021**, *43*, 11–25.
9. Yan, B.; Wang, P.; Ren, F.; Guo, Q.; Cai, M. A review of mechanical properties and constitutive theory of rock mass anisotropy. *Arab. J. Geosci.* **2020**, *13*, 487. [CrossRef]
10. Luo, M.; Gao, D.L.; Huang, H.L.; Li, J.; Yang, H.W.; Zhang, G.; Liu, K. Influence of drilling fluid on shale mechanical properties and wellbore stability. *Oil Drill. Prod. Technol.* **2022**, *44*, 693–700.
11. Zhou, X.; Liu, X.; Liang, L. Analysis of changes in shale mechanical properties and fault instability activation caused by drilling fluid invasion into formations. *J. Pet. Explor. Prod. Technol.* **2024**, *14*, 2343–2358. [CrossRef]
12. Wang, H.; Feng, F.; Zhang, J.; Han, X.; Zhang, Y.; Zhang, K. Effects of drilling fluid intrusion on the strength characteristics of layered shale. *Heliyon* **2025**, *11*, e42878. [CrossRef]
13. Liu, H.B.; Sun, H.R.; Cui, S.; Wang, S.; Du, S. Study on deformation mechanism and mechanical properties of bedding shale. *Chin. J. Undergr. Space Eng.* **2023**, *19*, 174–180.
14. Geng, D.D.; Qi, X.Y.; Fu, P.; Wang, S.W.; Ke, T. Mechanical properties and damage constitutive model of shale under different drilling fluid immersion conditions. *Coal Sci. Technol.* **2023**, *51*, 109–118.
15. Wang, J.M.; Zhang, S. Degree and influence of drilling fluid invasion in ultra-low permeability sandstone reservoirs. *Acta Pet. Sin.* **2019**, *40*, 1095–1103.
16. Dong, L.; Wu, N.Y.; Leonenko, Y.; Wan, Y.; Liao, H.; Hu, G.; Li, Y. A coupled thermal-hydraulic-mechanical model for drilling fluid invasion into hydrate-bearing sediments. *Energy* **2023**, *278*, 127785. [CrossRef]
17. Deng, F.Y. Study on the Law of Drilling Fluid Invasion into Shale Formations and its Influence on Wellbore Stability. Master's Thesis, Southwest Petroleum University, Chengdu, China, 2019.
18. Li, P.; Wang, Y.; Liu, J.; Li, P. Evaluation of Carbon Emission Efficiency and Analysis of Influencing Factors of Chinese Oil and Gas Enterprises. *Energy Sci. Eng.* **2025**, *13*, 1156–1170. [CrossRef]
19. Li, H.; Wang, Q.; Zhang, K.; Zhang, Q.H.; Song, T.; Zhang, C.; Zhuo, L.B.; Hao, C.; Feng, F.P.; Wang, H.; et al. The invasion law of drilling fluid along bedding fractures of shale. *Front. Earth Sci.* **2023**, *11*, 1112441. [CrossRef]
20. Suo, Y.; Li, F.F.; He, W.Y.; Fu, X.F.; Pan, Z.J.; Feng, F.P.; Zhao, W.C. A model of drilling fluid invasion into laminated shale. *J. Eng. Sci.* **2024**, *46*, 547–555.
21. Wang, H.Y.; Feng, F.P.; Zhang, J.W.; Han, X.; Zhang, Y.H.; Zhang, K. Impact of rock strength degradation by fluid intrusion on borehole stability in shale. *Nat. Gas Ind. B* **2024**, *11*, 553–568. [CrossRef]

22. Ma, T.S.; Chen, P. Wellbore stability analysis of horizontal wells in bedding shale. *J. Cent. South Univ. Nat. Sci. Ed.* **2015**, *46*, 1375–1383.
23. Saroglou, H.; Tsiambaos, G. A modified Hoek–Brown failure criterion for anisotropyic intact rock. *Int. J. Rock Mech. Min. Sci.* **2008**, *45*, 223–234. [CrossRef]

Disclaimer/Publisher's Note: The statements, opinions and data contained in all publications are solely those of the individual author(s) and contributor(s) and not of MDPI and/or the editor(s). MDPI and/or the editor(s) disclaim responsibility for any injury to people or property resulting from any ideas, methods, instructions or products referred to in the content.